International Journal of Multidisciplinary Research and Growth Evaluation.

The change material mechanical properties based on elastic-viscous material model

Ho Duy Khanh [1*], Bui Sy Vuong [2], Mach Thi Bich Ngoc [3], Nguyen Thi Hoa Cuc [4], Thanh Q Nguyen [5]
[1, 5] Faculty of Engineering and Technology, Thu Dau Mot University, Binh Duong Province, Vietnam
[3] Electronic Engineering Program, Faculty of Engineering and Technology, Thu Dau Mot University, Binh Duong Province, Vietnam
[4] Automotive & Mechatronics Program, Faculty of Engineering and Technology, Thu Dau Mot University, Binh Duong Province, Vietnam
[2] Institute of Southeast Vietnamese Studies, Thu Dau Mot University, Binh Duong Province, Vietnam

* Corresponding Author: **Bui Sy Vuong, Mach Thi Bich Ngoc, Nguyen Thi Hoa Cuc, Nguyen Q Thanh**

Article Info

ISSN (online): 2582-7138
Volume: 03
Issue: 04
July-August 2022
Received: 02-06-2022
Accepted: 19-06-2022
Page No: 98-108
DOI: https://doi.org/10.54660/anfo.2022.3.4.2

Abstract
The manuscript proposes to use the elastic-viscous material model to simulate the process of changing the mechanical state of the material during operation time. The proposed model established a link between the mechanical properties of the material and the structure's operation. Material mechanical parameters are represented by two parameters: elastic modulus and viscous drag coefficient. The structure's performance evaluation parameter is represented by two kinetic parameters during vibration, namely natural frequency and forced vibration amplitude. The novel aspect of this study is the inclusion of a viscous drag coefficient in the mechanical properties of materials to compensate for the shortcomings of previous evaluation models that are not consistent with reality. This research allows for a more in-depth examination of the material's mechanical properties as well as its ability to change over the course of the structure's life. The study improved some kinetic characteristics related to the material's operation by increasing the number of parameters of the viscosity coefficient in the mechanical properties of the material.

Keywords: Material mechanics, structural mechanics, elastic-viscous material model, viscous drag coefficient

1. Introduction

Traffic works are always important in all societal activities. The failure of the bridge not only causes traffic delays and significant economic loss, but it can also result in personal injury. As a result, monitoring the operational status of the structure is a continuous task of traffic management agencies in order to ensure absolute safety during operation. As a result, the problem of diagnosing structural damage has received a lot of attention in recent years [1-5]. According to research, the weakening process is typically represented by the presence of defects or deterioration of the structure. This is a process that is affected by unforeseen factors in the design process such as vehicle growth rate, weather, environmental factors such as sunlight, heat, high humidity, and natural disasters. In the problem of determining defects in the structure through basic elements such as piles, shafts, pipes, beams, slabs, and spans. In which the spectral model of the structure and the finite element method are the most widely used in most measures to evaluate the structure's change.

Mechanically, a structure's weakening mechanism can be divided into structural stiffness deterioration [6-7] and material stiffness reduction due to internal material molecule bonding [8-10]. As a result, the general trend of research on this topic can be divided into two main research directions: structural and unstructured.

Non-structural methods of analysis are typically used in the problem of structural change [11-13]. The results of structural change evaluation are typically calculated using actual measurement signals [14-16]. In which the parameters representing the individual state of each mechanical work will be used to assess the structure's condition during operation. This means that we can completely assess the structure's damage by determining the change of those parameters without using mathematical models.

This unstructured method has the benefit of avoiding mistakes and subjective errors when modeling specific structures. These

problems can greatly affect the evaluation process such as calculation errors and processing time. The disadvantage of the unstructured method is that it is difficult to locate and assess the degree of structural damage.

In contrast, structural studies concentrate on modeling methods for connecting theoretical and empirical models. This allows for the identification and prediction of the failure process by determining the relationship between the structure and the defect. The most significant advantage of these studies is that they provide an accurate result about the relationship between the structure's behavior and each type of defect. At the same time, this method can forecast the occurrence and rate of progression of defects in the future.

The bridge structure is the group of structures prioritized for monitoring and evaluation among typical structures. The span and pier are the basic and main force-bearing elements of the bridge [17-19]. The span of the bridge is usually much longer than the other dimensions, for example, because the slab structure used in the deck slab is reinforced and reinforced by the beams below. As a result, the span structure is frequently modeled as a bearing beam connected at both ends in many mechanical problems. In applied research for actual bridge spans, two beam models are commonly used: Euler-Bernoulli beam theory [20-22] and Timoshenko beam theory [23-25]. When we ignore the influence of shear deformation and rotational inertia of the cross section, the Euler-Bernouli beam model is a special case of the Timoshenko beam [20, 24]. According to [28-30], research based on natural frequency and vibration pattern criteria to compare the fit between the Euler-Bernouli and Timoshenko beam models via the two-dimensional element in the elastic domain. With vibration patterns of practical importance such as bending and torsional vibrations, the results show that the Timoshenko beam theory is more similar to the two-dimensional element theory than the Euler-Bernouli theory. Furthermore, the Timoshenko beam theory is applicable to short beams with girder lengths greater than 15 times the beam height, whereas the Euler-Bernouli theory [22, 21], which is applicable to long beams, is less commonly used in research. The authors [27, 26, 6, 18] compared the theoretical results of the natural frequencies of two models of Euler-Bernouli and Timoshenko beams with cracks and demonstrated that the influence of cracks on the natural frequencies of the two models is not different if the ratio of the two models is not different. The girder length and height are both greater than ten. However, many authors believe that, while the Timoshenko beam model has significantly improved over the Euler-Bernouli model, there are still many unsatisfactory problems, and thus the Euler-Bernouli beam model will continue to be used. popular and widely used, as well as for the problem of beam bending vibration Furthermore, the Euler-Bernouli beam model is used in the majority of studies on the interaction of traffic loads and bridge structures. In fact, abnormal fluctuations in the environment have an impact on material factors such as construction technology, the environment, and loads. We discovered that the mechanical properties of the material will change before cracks appear in the structure. As a result, using material mechanical models to calculate damage and predict the occurrence of defects in structures is an urgent and necessary need. As a result, the construction of a method to determine the relationship between the theoretical model and the experimental model in the material mechanical change model is still limited in practice. Special properties of materials, or specific materials, make providing solutions to the technical problems involved difficult. Material property research is gradually becoming more sophisticated. This will pave the way for most modern engineering disciplines around the world, particularly in construction measurement and monitoring.

To address the shortcomings of previous studies, the manuscript used an elastic-viscous model to represent the material's mechanical behavior. The study creates a working model of the bridge span structure using Timoshenko's beam model in conjunction with the elastic-viscous material model. The manuscript's proposed model has many advantages over previous models because it shows the relationship between two mechanical parameters of the material, including elastic modulus and viscous drag coefficient. Concurrently combined with two kinematic parameters shown during the structure's vibration, including natural frequency and forced vibration amplitude. This study is unique in that it not only proposes including the viscosity coefficient C_0 in the mechanical properties of materials to compensate for the deviations of previous evaluation models, but it also allows monitoring the change of mechanical properties of materials over time. The research allows for a more in-depth examination of the material's mechanical properties as well as its ability to change over the course of the structure's life. Although the study only presents one case of a single bending beam with two ends bearing a harmonic variable force of constant amplitude, the study's applicability is vast; it can be applied to many different material models in practice.

2. Theoretical basis

2.1. Elastic-viscous material modeling

When calculating the strength of materials, buildings are frequently modeled as simple diagrams with the stress and deformation of the material removed. Hooke's law, in particular, is only used for materials that are considered linearly elastic because it ignores creep and stress relaxation phenomena, but the calculation process is still very complicated and results in errors. The obtained results are incorrect. The creep phenomenon is regarded as the aging process of materials, implying that their deformation will increase under constant load. Furthermore, the stress is now understood that when the stress is reduced, the strain remains constant. These are two distinct characteristics of elastic-viscous bodies. When the strain on these objects increases, stresses appear with the following characteristics: depending on the deformation and the rate of development of the deformation. Elastic-viscous materials are commonly used in a wide range of construction structures. This material model can easily control unforeseen vibrations and noise propagation. Establishing stress-strain relationships for viscoelastic materials is critical for defect detection. This model can also be applied to objects that, even with minor deformations, do not obey Hooke's law [31]. The curve Eq.(1), which represents internal frictional forces, represents the physical law between stress and strain. As shown in Fig. 1, the properties of elastic bodies (representing a linear spring) and viscous bodies (representing a shock absorber) receive a lot of attention in engineering.

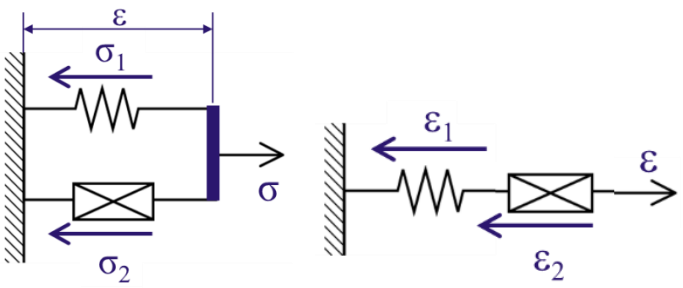

(A) Parallel (B) Series

Fig 1: Internal friction force model at a material element

And, as shown in Figs. 1a-b, the stress and strain at a material element of viscoelastic materials are calculated as follows:

$$\sigma = \sigma_1 + \sigma_2 \tag{1}$$

$$\varepsilon = \varepsilon_1 + \varepsilon_2 \tag{2}$$

With $\sigma_1 = E\varepsilon$ and $\varepsilon_1 = \sigma / E$, linear friction component, there is no damping, σ_2 and ε_2 are the friction component that causes energy loss, representing internal force and deformation with non-linear components. The advantages of elastic-viscous models are that they demonstrate the common practical behavior characteristics of materials. Following that, we will look at the time and frequency domain behavior of the elastic - viscous model.

2.2. Creating the beam model's flexural vibration equation with elastic-viscous materials

Consider a beam element that is bent as a result of an external force *f*

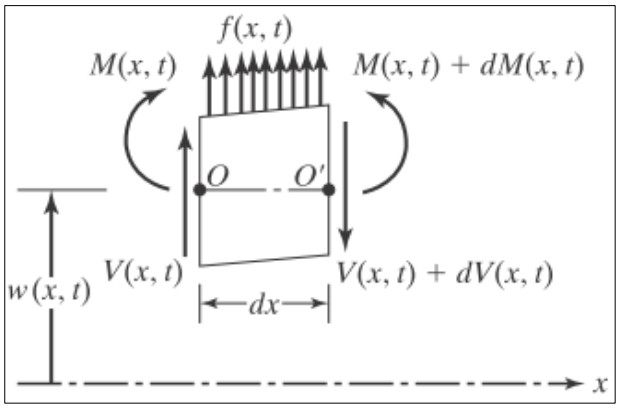

Fig 2: Bending vibration model of beams

When the body is subjected to bending deformation, the moment and force balance equation

$$(M + dM) - (V + dV)dx + f(x,t)dx\frac{dx}{2} - M = 0 \tag{3}$$

$$-(V + dV) + f(x,t)dx + V = \rho A(x)dx\frac{\partial^2 w}{\partial t^2}(x,t) \tag{4}$$

We represent: $dV = \frac{\partial V}{\partial x}dx \; ; dM = \frac{\partial M}{\partial x}dx$ (5)

When we substitute formula (5) into Eq. (3) and Eq. (4) and remove the higher order infinitesimal

$$\frac{\partial M(x,t)}{\partial x} - V(x,t) = 0 \tag{6}$$

$$-\frac{\partial V(x,t)}{\partial x} + f(x,t) = \rho A(x)\frac{\partial^2 w}{\partial t^2}(x,t) \tag{7}$$

Continually substituting *V(x,t)* from Eq. (6) to Eq. (7), as shown in Eq.(8)

$$-\frac{\partial^2 M(x,t)}{\partial x^2}+f(x,t)=\rho A(x)\frac{\partial^2 w}{\partial t^2}(x,t) \tag{8}$$

We have the relationship between the radius of curvature *r* of the beam and the deflection *w* of the beam as follows:

$$\partial x = r\partial\varphi \Rightarrow \frac{1}{r}=\frac{\partial\varphi}{\partial x}=\frac{\partial^2 w}{\partial x^2} \tag{9}$$

Then the strain at position y on the cross-section with radius r is determined:

$$\varepsilon = -\frac{1}{r}y \tag{10}$$

According to the elastic-viscous model, the shear stress σ appearing on a material element when the object has a long strain ε will have the form:

$$\sigma = E\varepsilon + C_0\frac{\partial\varepsilon}{\partial t} \tag{11}$$

Substituting Eq. (10) into Eq. (11) we have: $\sigma = -E\frac{1}{\rho}y - C_0\frac{\partial}{\partial t}\left(\frac{1}{\rho}y\right)$ (12)

In the long strain of the material, *E* is the elastic modulus and C_0 is the coefficient of viscous drag. The internal force moment at cross-section *x* can then be calculated as follows:

$$M = \int_A \sigma y dA \tag{13}$$

Substituting Eq. (11) and Eq. (12) into Eq. (13)

$$\begin{aligned} M &= -E\frac{1}{\rho}\int_A y^2 dA - C_0\frac{\partial}{\partial t}\left(\frac{1}{\rho}\right)\int_A y^2 dA \\ M &= -EJ\frac{\partial^2 w}{\partial x^2} - C_0 J\frac{\partial}{\partial t}\left(\frac{\partial^2 w}{\partial x^2}\right) \end{aligned} \tag{14}$$

Substituting Eq. (14) into Eq. (7), we have the equation of torsional vibration of the shaft as follows:

$$EJ\frac{\partial^2 w}{\partial x^4}+C_0 J\frac{\partial^5 w}{\partial x^4\partial t}+\rho A\frac{\partial^2 w}{\partial t^2}=f(x,t) \tag{15}$$

2.2.1 Response to bending vibration

The separation of variables method is the general method for solving multivariable differential equations:

$$w=\sum_{r=1}^{n} w_r = \sum_{r=1}^{n} W_r(x)T_r(t) \tag{16}$$

$$\begin{aligned} f(x,t) &= \sum_{r=1}^{n} W_r(x)h_r(t) \\ h_r(t) &= \frac{\int_0^l f(x,t)W_r(x)dx}{\int_0^l W_r^2(x)dx} \end{aligned} \tag{17}$$

Wr(x) must be eigenforms that satisfy the boundary conditions in order for *hr(t)* to be computed in terms of Eq. (16), so the *Wr(x)* must be chosen to satisfy the boundary condition. We get the following by substituting the solution form Eq. (16) and the split form of the external force Eq. (17) into the bending vibration equation as shown in Eq. (14):

$$\frac{EJ}{\rho A}W_r^{(4)}T_r + \frac{c_0 J}{\rho A}W_r^{(4)}\dot{T}_r - W_r\ddot{T}(t) = \frac{W_r h_r}{\rho A} \tag{18}$$

Transform Eq. (18) we get: $$\frac{EJ}{\rho A}W_r^{(4)}\left(T_r + \frac{C_0}{E}\dot{T}_r\right) = W_r\left(-\ddot{T}_r + \frac{h_r}{\rho A}\right) \tag{19}$$

Eq. (7) allows to set up two equations as shown in Eq. (20) and Eq. (21):

$$W_r^{(4)} - p_r{}^2\frac{\rho A}{EJ}W_r = 0 \tag{20}$$

$$\ddot{T}_r + p_r{}^2\frac{C_0}{E}\dot{T}_r + p_r{}^2 T_r = \frac{h_r}{\rho A} \tag{21}$$

The function *Wr(t)* must be chosen to satisfy the boundary condition while also satisfying both the boundary condition and the system of homogeneity equations written from differential equations as in Eq. (20). The Eq. (10) indicates that converting from the coordinate system *w(x,t)* to the coordinate system $T_r(t)$, with $r = 1,2...\infty$ will make the calculation process easier. This has significant practical implications because it reduces the problem of investigating systems with infinitely many degrees of freedom to a set of problems examining systems with one degree of freedom. We can see from the above transformation that the displacement *w* at each position *x* is a combination of time-varying motions *t* according to the functions $T_r(t)$. We can conclude that in order to investigate the influence of mechanical parameters on *w(x,t),* we must first investigate their influence on the function $T_r(t)$. Equation (21) shows that it is completely consistent with the damped 1-degree-of-freedom mechanical model:

$$\ddot{T}_r + 2n\dot{T}_r + p^2 T_r = h_0 \sin\omega t \tag{22}$$

With $$p_r{}^2\frac{C_0}{E} = 2n; p_r^2 = p^2; \frac{h_r(t)}{\rho A} = h_0 \sin\omega t \tag{23}$$

Stable solution of Eq. (22): $$T_r = \mathrm{A}\sin(\omega t - \varphi) \tag{24}$$

In there: $$A = \frac{h_0/p^2}{\sqrt{\left[1-\left(\frac{\omega}{p}\right)^2\right]^2 + 4\left(\frac{\omega}{p}\right)^2\left(\frac{n}{p}\right)^2}} \tag{25}$$

With: p – natural frequency; ω – forced frequency. According to Eq. (24), the amplitude value A depends on the dynamic coefficient for the same load amplitude μ (amplification factor or shock coefficient).

With: $$\mu = \frac{1/p^2}{\sqrt{\left[1-\left(\frac{\omega}{p}\right)^2\right]^2 + 4\left(\frac{\omega}{p}\right)^2\left(\frac{n}{p}\right)^2}} \tag{27}$$

2.2 Applying elastic-viscous material model for bridge span

Some spans are longer than others and are reinforced by lower beams with two ends supported by piers. Because the circulating load primarily exerts force perpendicular to the span, the span becomes the primary flexural force, allowing a span model to be converted into a double-ended supporting beam, as shown in Fig. 3.

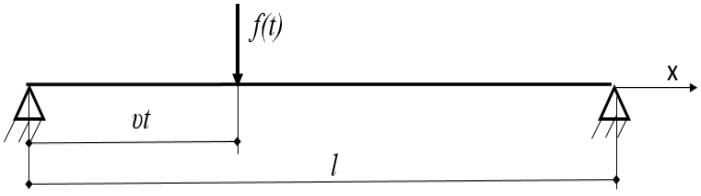

Fig 3: Model of a simply supported beam is bearing the force perpendicular to the beam

Then there are parameters like the eigenform function and the natural frequency of the beam with the two-headed connection, which have the form

$$p_r = \frac{r^2 p^2}{l^2}\sqrt{\frac{EJ}{rA}} \qquad j = 1,2,....,n \tag{28}$$

$$W_r(x) = \sin(r\pi\frac{x}{l}) \tag{29}$$

Assume that the time-varying force function *f(t)* in Eq. (7) has the basic form of a harmonic function as shown in Eq.(30)

$$f(t) = q_0 \sin(\omega t) \tag{30}$$

Substituting Eq. (29) into Eq. (16)

$$h_r = \frac{4q_0}{r\pi} \tag{31}$$

According to Eq. (24), the amplitude of the forced solution

$$A_r = \frac{4q_0}{r\pi\rho A p_r^2}\frac{1}{\sqrt{\left[1-\left(\frac{\omega}{p_r}\right)^2\right]^2+\left(\frac{C_0\omega}{E}\right)^2}} \tag{32}$$

When $\omega=p_r$, the amplitude value A_r reaches the maximum value $A_{r,\,max}$ is called the resonance amplitude of the r^{th} harmonic.

From Eq.(31), $A_{r,\max} = \frac{4q_0}{r\pi\rho A p_r^3}\frac{E}{C_0} = \frac{1}{r^7}\frac{1}{C_0}\sqrt{\frac{\rho A}{EJ^3}}\frac{4q_0 l^6}{\pi^7}$ (33)

Examine the effects of harmonic order r, elastic modulus E, viscous drag coefficient C_0, and vibration amplitude A_r on natural frequency p_r and vibration amplitude A_r

3. Results and discussion

3.1. Examine the characteristics of natural frequency variation

According to Eq. (33), the natural frequency value proportional to the square of the harmonic order, i.e. proportional to r^2, is shown as Eq. (28). This means that in the case of a single girder connection, if the first natural frequency is 3Hz, the next frequencies will be 12 Hz, 27 Hz, 48 Hz, and 75 Hz, increasing by a multiple of r^2 times. Taking only the fifth natural frequency into account, it is already 25 times higher than the first natural frequency. Fig. 4 depicts the change in natural frequencies as a result of the viscoelastic model.

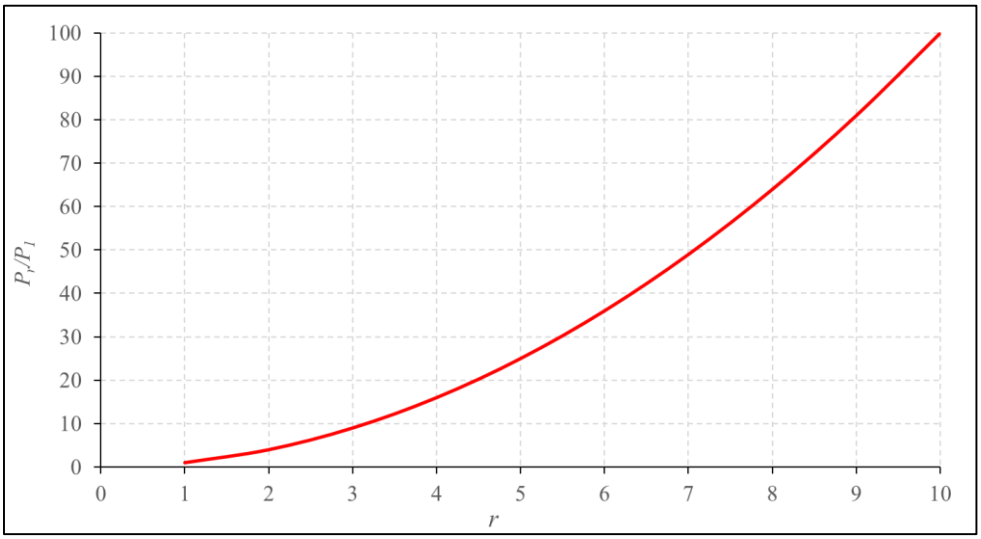

Fig 4: The natural frequency change ratio based on the natural form of the bending vibration

The model used to investigate this result, and the results from Table 1 and Table 2 show that, while the phenomenon of changing natural frequency values in the beam model cannot be explained, the law of change change completely according to the model shape of viscous material

Table 1: The natural frequencies of the beam model with free-free boundary conditions

Length of crack (mm)	Position of crack (m)	Natural frequency	f_1 (Hz) (Hz)	f_2 (Hz) (Hz)	f_3 (Hz) (Hz)	f_4 (Hz) (Hz)
0	Intact	[32]	55.52	152.97	299.69	494.97
		[33]	56.75	156.39	306.19	506.15
		[17]	55.52	222.08	499.68	888.32
		Present	55.50	222.10	500.12	888.45
1	0.375	[32]	55.04	150.08	296.69	493.51
		[33]	56.38	156.30	305.47	506.02
		[17]	55.36	221.44	498.24	885.76
		Present	55.41	221.45	499.50	885.88
3	0.375	[32]	53.79	148.96	292.69	485.07
		[33]	54.31	156.08	296.34	504.54
		[17]	53.76	215.04	483.84	860.16
		Present	53.77	215.12	485.12	866.24

Table 2: The natural frequencies of the beam model with fixed-free boundary conditions

Length of crack (mm)	Position of crack (m)	Natural frequency	f_1 (Hz) (Hz)	f_2 (Hz) (Hz)	f_3 (Hz) (Hz)
0	Intact	[32]	7.70	48.25	135.05
		[34]	7.68	47.17	134.81
		[17]	7.70	30.81	69.31
		Present	7.71	30.92	69.50
1.8	0.4	[32]	7.69	47.90	133.13
		[34]	7.60	46.87	130.21
		[17]	7.50	30.00	67.52
		Present	7.49	30.10	67.54
2.4	0.4	[32]	7.58	46.59	131.05
		[34]	7.46	46.16	129.28
		[17]	7.45	29.82	65.05
		Present	7.44	30.01	65.15

According to Timoshenko's beam theory, the natural frequency value is only affected by the elastic modulus E, as shown by Eq. (28), but not by the viscous drag coefficient C_0. Fig. 5 depicts the degree of variation for p_r as a function of variability E.

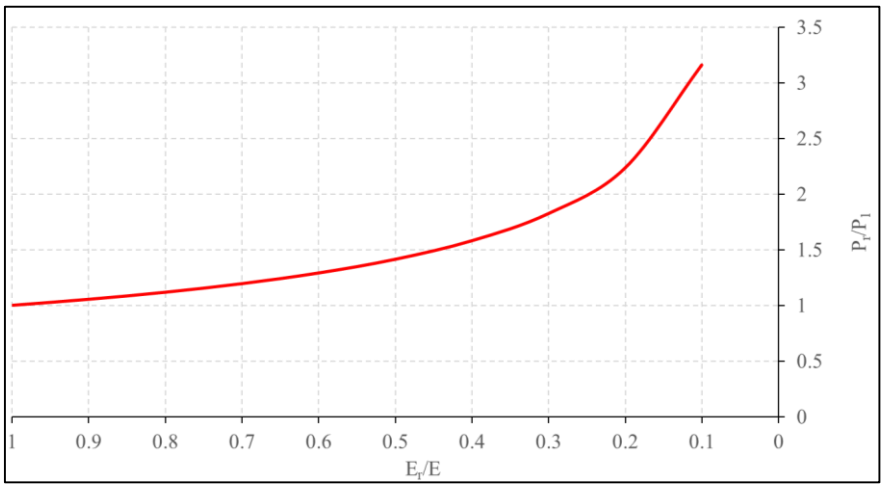

Fig 5: Relationship of natural frequency variation according to elastic modulus

This means that the elastic modulus of the structure will decrease over time due to brainening, fatigue, or stretching of the material during operation. Fig. 5 shows that when the overall elastic modulus is reduced by nearly 20% compared to the original value, the change in the natural frequency value of the structure is reduced by only about 10%. With actual structure lives typically measured in years, it takes a very long time for the structure to change 10% of its elastic modulus value.

2.4. Examine the variation in resonance amplitude

- According to Eq. (33), $A_{r,max}$ is inversely proportional to the 7^{th} power of r. This means that the larger the amplitude of the harmonics with the order number, the smaller the value of the resonance amplitude, which means a very large attenuation.

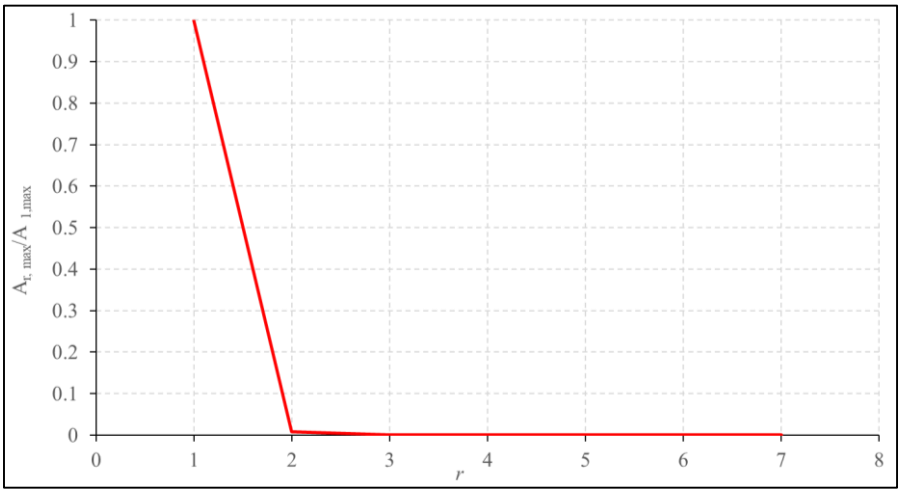

Fig 6: Resonance amplitude attenuation of high frequency harmonics

According to Fig. 6, the bending vibration of a simple two-headed beam using the Timoshenko model, the amplitude of the higher harmonics ($r > 2$) is typically very small in comparison to the amplitude of the first harmonic. As a result, we can only detect the first type of vibration using the vibration measurement data of the bridge girder, which is difficult to detect because the amplitude is almost negligible and easily misinterpreted. in combination with signal interference
$A_{r,\,max}$ is also inversely proportional to the viscosity coefficient C_0, according to Eq. (33). In practice, the change in mechanical properties shows that C_0 increases, resulting in a decrease in the amplitude $A_{r,\,max}$ with time, as shown in Fig. 7.

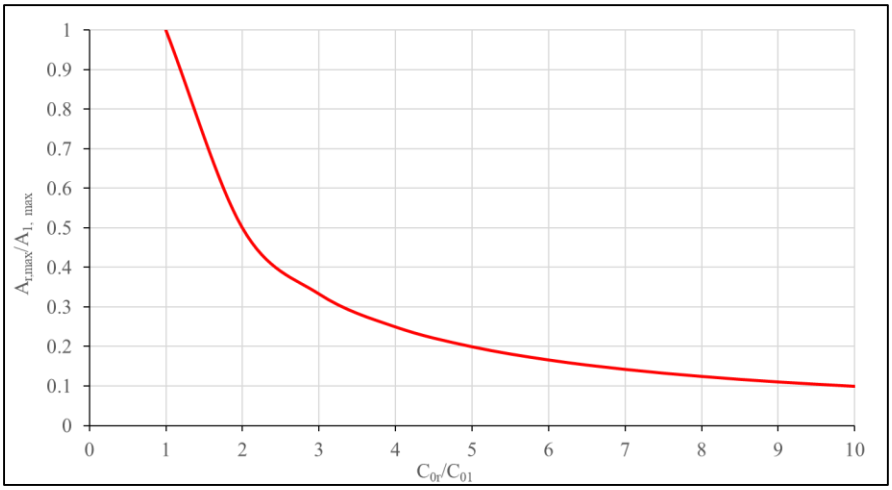

Fig 7: The attenuation of the resonance amplitude of the harmonics according to the viscous drag coefficient

$A_{r,max}$ is also inversely proportional to the square root of the elastic modulus E, according to Eq. (33). In fact, many studies show that the elastic modulus changes as mechanical properties change. Then the amplitude $A_{r,max}$ will increase over time. Combining the previous comments, we can draw the following conclusions: if the time $A_{r,max}$ increases, the elastic modulus E decreases, and if the time $A_{r,max}$ decreases, the viscosity coefficient C_0 increases.

3. Experimental verification

Fig. 8 depicts the experimental data surveyed, which is the vibration data of the span of the 31 Saigon bridge at various times of survey.

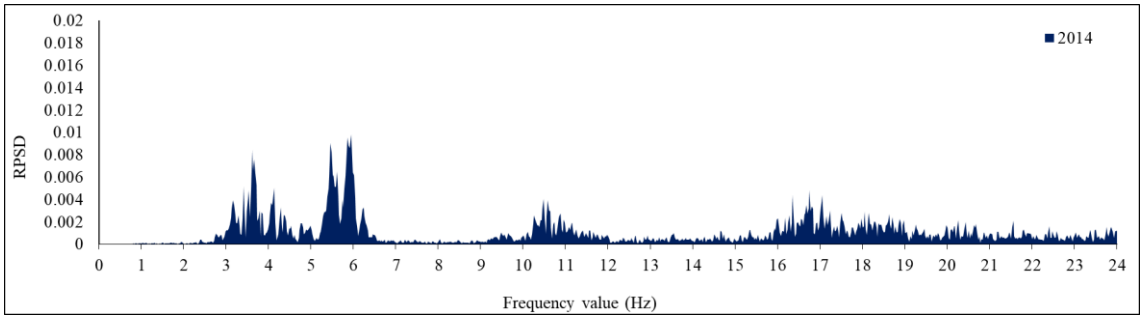

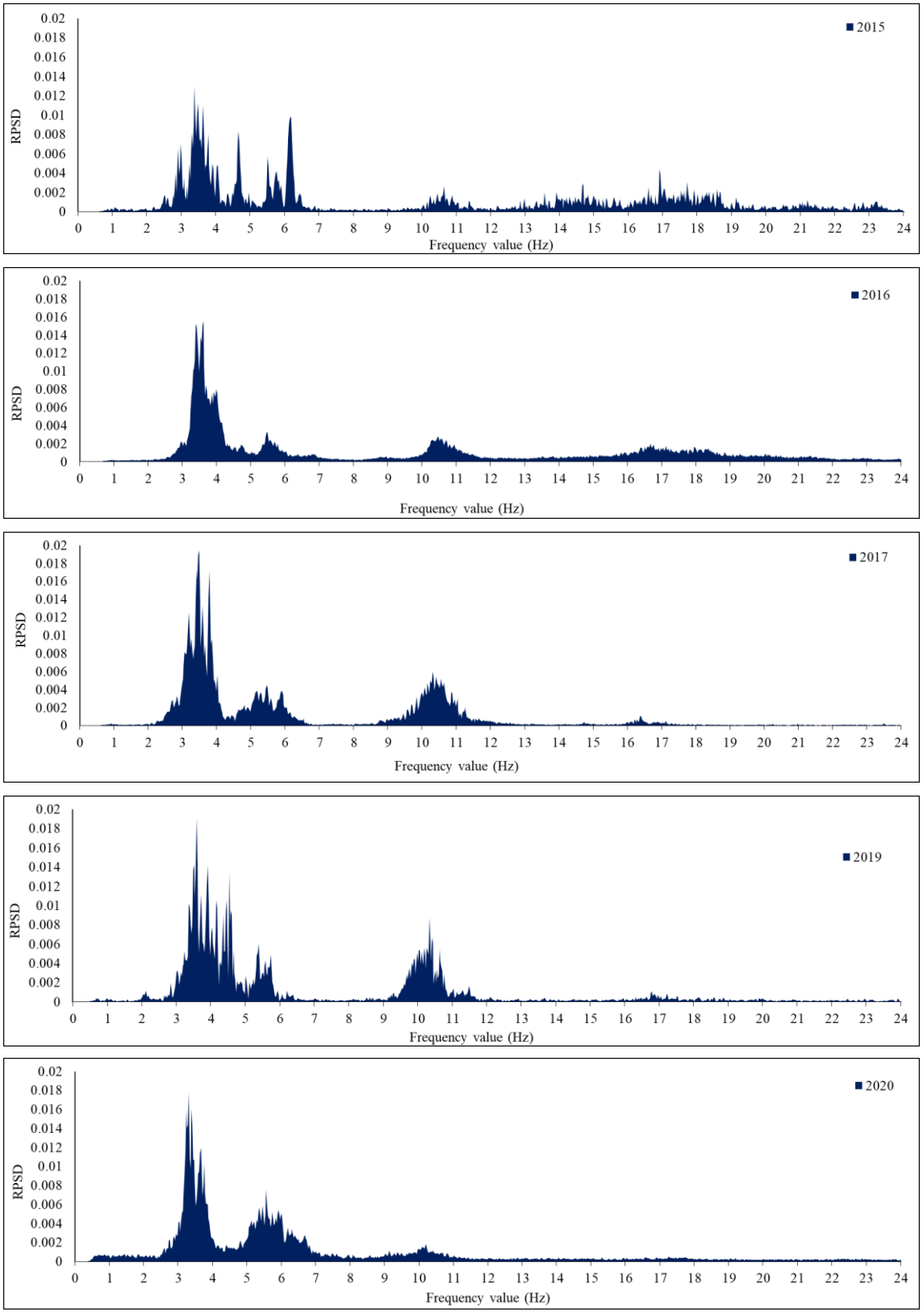

Fig 8: Vibration spectrum of the 31 Saigon Bridge span at different times

The amplitude of harmonics in the high frequency region will be less than that of harmonics in the low frequency region. This is consistent with the statements in Eq. (32), so the amplitude value of the harmonics is inversely proportional to the order of the vibration patterns present in the structure. The resonance amplitudes of the regions decrease over time due to mechanical changes in the material, such as fatigue, creep, and brainization. As a result of this changing process, the viscous drag coefficients of these harmonics increase, as demonstrated by Eq. (33)

- Over time, the peaks of some resonance regions occasionally increase, contradicting previous judgments; this can be explained by the load acting on the bridge span at the time of survey, as well as environmental influences such as temperature, wind, and humidity. It can be seen that the elastic modulus of the material structure decreases during this time. However, in the overall process of spectral amplitude change, the majority of these amplitudes have attenuation from low

to high frequency region. Because of the shifting of frequency harmonics in the spectrum, the higher frequency region will have a faster attenuation amplitude than the lower regions. As a result, the value of viscous drag coefficient C_0 increased significantly more than the decrease in elastic modulus of the material during the survey period of the Saigon bridge vibration.

- The change in A_r amplitudes in the spectrum is more pronounced than the change in natural frequency value. This is consistent with theory, in which the natural frequency is only influenced by elastic modulus E, whereas the amplitude A_r shown in Eq. (33) is always influenced by elastic modulus E and the value of viscosity coefficient C_0.

4. Conclusion

The mechanical behavior of the material was represented by an elastic-viscous model in the manuscript. The study examines the relationship between two mechanical properties of materials: elastic modulus and viscous drag coefficient. Simultaneously combined with two kinematic parameters displayed during the structure's vibration, including natural frequency and forced vibration amplitude. The addition of the viscous drag coefficient C_0 in the mechanical properties of materials to compensate for the deviations of the previous evaluation models is the study's novelty. The study allows a more comprehensive investigation of the material's mechanical properties as well as its ability to change during the life of the structure. The study improved some kinetic characteristics related to the material's operation by increasing the number of C_0 parameters in the material's mechanical properties. Despite the fact that the study only presents one case of a single bending beam with two ends and a harmonic variable force of constant amplitude, it makes some important observations:

- Using the coefficient of viscous resistance improves the ability to evaluate and recognize changes in material mechanical properties. Because the amplitude parameter is dependent on both mechanical parameters of the material, it has a high potential in the failure identification problem. When the actual vibrations are compared to the theory, they are found to be quite consistent. This fit demonstrates that the elastic-viscous model can be used to describe the mechanical behavior of materials in the structural failure identification problem. It is more efficient to combine both vibration parameters than to use only one to realize the variation of the material's mechanical properties. This opens up a new avenue for establishing the failure identification process.
- Although using two parameters allows for better identification, quantitative analysis reveals that the number of individual vibration patterns seen in reality is extremely limited. This is a significant difficulty to recognize when studying measures and algorithms that diagnose on the basis of the vibrations' "own" characteristics on the basis of data obtained from the measurement.

5. Declaration of Interest statement

This is to certify that to the best of authors' knowledge, the content of this manuscript is original. The paper has not been submitted elsewhere nor has been published anywhere.

Authors confirm that the intellectual content of this paper is the original product of our work and all the assistance or funds from other sources have been acknowledged.

6. Data availability

All data generated or analysed during this study are included in this published article (and its supplementary information files).

7. Acknowledgment

This research is funded by Thu Dau Mot University, Binh Duong Province, Vietnam under grant number DT.21.2.068

8. References

1. Salawu OS. Detection of structural damage through changes in frequency: A review. Engineering Structures. 1997;19(9):718-723.
2. Sung SH, Jung HJ, Jung HY. Damage detection for beam-like structures using the normalized curvature of a uniform load surface. Journal of Sound and Vibration. 2013;332(6):1501-1519.
3. Xiang J, Matsumoto T, Wang Y, Jiang Z. Detect damages in conical shells using curvature mode shape and wavelet finite element method. International Journal of Mechanical Sciences. 2013;66:83-93.
4. Surace C, Bovsunovsky A. The use of frequency ratios to diagnose structural damage in varying environmental conditions. Mechanical Systems and Signal Processing. 2020;136:106523.
5. Adams DE, Farrar CR. Classifying linear and nonlinear structural damage using frequency domain ARX models. Structural Health Monitoring. 2002;1(2):185-201.
6. Nguyen TQ, Vuong LC, Le CM, Ngo NK, Nguyen-Xuan H. A data-driven approach based on wavelet analysis and deep learning for identification of multiple-cracked beam structures under moving load. Measurement. 2020;162:107862.
7. Nguyen TQ, Tran LQ, Nguyen-Xuan H, Ngo NK. A statistical approach for evaluating crack defects in structures under dynamic responses. Nondestructive Testing and Evaluation. 2021;36(2):113-144.
8. Lommen S, Lodewijks G, Schott D. DEM speedup: Stiffness effects on behavior of bulk material. Particuology. 2014;12:107-112.
9. Patton R, Li F, Edwards M. Causes of weight reduction effects of material substitution on constant stiffness components. Thin-Walled Structures. 2004;42(4):613-637.
10. Basri R, Chiu WK. Numerical analysis on the interaction of guided Lamb waves with a local elastic stiffness reduction in quasi-isotropic composite plate structures. Composite Structures. 2004;66(1-4):87-99.
11. Nguyen TQ, Nguyen TD, Nguyen-Xuan H, Ngo NK. A correlation coefficient approach for evaluation of stiffness

degradation of beams under moving load. CMC: Computers, Materials & Continua. 2019;61(1):27-53.
12. Nguyen HB, Nguyen TQ. Detecting and evaluating defects in beams by correlation coefficients. Shock and Vibration. 2021;2021:6536249.
13. Ngo NK, Nguyen TQ, Vu TV, Nguyen-Xuan H. A fast Fourier transform–based correlation coefficient approach for structural damage diagnosis. Structural Health Monitoring. 2020;19(2):1475921720949561.
14. Piazzaroli Finotti R, Abrahão Cury A, de Souza Barbosa F. An SHM approach using machine learning and statistical indicators extracted from raw dynamic measurements. Latin American Journal of Solids and Structures. 2019;16(2):1-17.
15. Ren WX, Sun ZS. Structural damage identification by using wavelet entropy. Engineering Structures. 2008;30(10):2840-2849.
16. Michaels JE, Michaels TE. Detection of structural damage from the local temporal coherence of diffuse ultrasonic signals. IEEE Transactions on Ultrasonics, Ferroelectrics, and Frequency Control. 2005;52(10):1769-1782.
17. Nguyen TD, Nguyen TQ, Nhat TN, Nguyen-Xuan H, Ngo NK. A novel approach based on viscoelastic parameters for bridge health monitoring: A case study of Saigon bridge in Ho Chi Minh City, Vietnam. Mechanical Systems and Signal Processing. 2020;141:106728.
18. Nguyen TQ, Nguyen TD, Tran LQ, Ngo NK. A new insight into vibration characteristics of spans under random moving load: Case study of 38 bridges in Ho Chi Minh City, Vietnam. Shock and Vibration. 2020;2020:1547568.
19. Li H, Li XZ, Zheng J. Vibration characteristics of fully enclosed sound barriers on railway bridges under the movement of trains. Advances in Civil Engineering. 2021;2021(1):2939504.
20. Bauchau OA, Craig JI. Euler-Bernoulli Beam Theory. Dordrecht: Structural Analysis. Solid Mechanics and Its Applications. Springer; c2009.
21. Civalek Ö, Demir Ç. Bending analysis of microtubules using nonlocal Euler–Bernoulli beam theory. Applied Mathematical Modelling. 2011;35(5):2053-2067.
22. Sumelka W, Blaszczyk T, Liebold C. Fractional Euler–Bernoulli beams: Theory, numerical study and experimental validation. European Journal of Mechanics - A/Solids. 2015;45:243-251.
23. Wang CM, Kitipornchai S, Lim CW, Eisenberger M. Beam bending solutions based on nonlocal Timoshenko beam theory. Journal of Engineering Mechanics. 2008;134(6):475-481.
24. Reddy JN, Wang CM, Lee KH. Relationships between bending solutions of classical and shear deformation beam theories. International Journal of Solids and Structures. 1997;34(26):3373-3384.
25. Gao XL. A new Timoshenko beam model incorporating microstructure and surface energy effects. Acta Mechanica. 2015;226:457-474.
26. Wang CM. Timoshenko beam-bending solutions in terms of Euler-Bernoulli solutions. Journal of Engineering Mechanics. 1995;121(6):763-765.
27. Lim CW, Wang CM, Kitipornchai S. Timoshenko curved beam bending solutions in terms of Euler-Bernoulli solutions. Archive of Applied Mechanics. 1997;67:179-190.
28. Grobbelaar-Van Dalsen M. Uniform stabilization of a nonlinear structural acoustic model with a Timoshenko beam interface. Mathematical Methods in the Applied Sciences. 2006;19(15):1749-1766.
29. Vosoughi AR. A developed hybrid method for crack identification of beams. Smart Structures and Systems. 2014;16(3):401-414.
30. Wang C, Tawfick S, Vakakis AF. Time scale disparity yielding acoustic nonreciprocity in a two-dimensional granular-elastic solid interface with asymmetry. Physical Review. 2021;104(4):044906.
31. Rychlewski J. On Hooke's law. Journal of Applied Mathematics and Mechanics. 1984;48(3):303-314.
32. Mehrjoo M, Khaji N, Ghafory-Ashtiany M. New Timoshenko-cracked beam element and crack detection in beam-like structures using genetic algorithm. Inverse Problems in Science and Engineering. 2014;22(3):359-382.
33. Khatir S, Dekemele K, Loccufier M, Khatir T, Abdel Wahab M. Crack identification method in beam-like structures using changes in experimentally measured frequencies and particle swarm optimization. Comptes Rendus Mécanique. 2018;346(2):110-120.
34. Jena PK, Parhi DR. A modified particle swarm optimization technique for crack detection in cantilever beams. Arabian Journal for Science and Engineering. 2015;40(1):3263-3272.